

Contribution from the Department of Applied Chemistry,  
Faculty of Engineering, Kumamoto University, Kurokami, Kumamoto 860, Japan

## Ab Initio MO Study of Palladium-Assisted Nucleophilic Attack on a Coordinated Olefin: Semiquantitative Understanding of the Reaction and the Mechanism of Palladium Acceleration

Shigeyoshi Sakaki,\* Katsuhiko Maruta, and Katsutoshi Ohkubo

Received January 6, 1987

Aminopalladation of olefins is theoretically investigated here as an example of palladium-assisted nucleophilic attack on a coordinated olefin by an ab initio MO method and energy decomposition analysis. In  $[\text{PdF}_3(\text{C}_2\text{H}_4)]^-$  and  $\text{PdF}_2(\text{NH}_3)(\text{C}_2\text{H}_4)$ , the trans attack of a nucleophile,  $\text{NH}_3$ , on the coordinated ethylene causes significant destabilization. In  $[\text{PdF}(\text{NH}_3)_2(\text{C}_2\text{H}_4)]^+$  and  $[\text{PdF}(\text{PH}_3)_2(\text{C}_2\text{H}_4)]^+$ , on the other hand, the trans attack of  $\text{NH}_3$  proceeds easily with a rather small activation barrier. These results suggest that the active species is a cationic palladium(II)-olefin complex. Analyses of the interaction energy and electron distribution indicate that not only charge transfer from the nucleophile,  $\text{NH}_3$ , to  $\text{C}_2\text{H}_4$  but also polarization of the  $\text{Pd}-\text{C}_2\text{H}_4$  moiety is important to the reaction. Orbital mixings for frontier orbitals proposed here clearly elucidate why the cationic complex accelerates nucleophilic attack but why both the neutral and anionic complexes hardly do and how the geometry and electronic structure change during the reaction.

### Introduction

While unactivated olefins do not undergo nucleophilic attack, their coordination to appropriate transition-metal ions can often accelerate the reaction.<sup>1</sup> Such metal-assisted nucleophilic attack is involved as a key step in many catalytic reactions and organic syntheses with transition metals.<sup>1,2</sup> In this type of nucleophilic attack, information about the origin of the acceleration by metal coordination, factors contributing to the activation of olefins, and changes in electron distribution and geometry during nucleophilic attack are important and useful in improving the reactivity of transition-metal complexes and in finding good catalysts for the nucleophilic attack. Some of these aspects can be effectively investigated with an MO method, and therefore, during the last decade several MO studies have been carried out on metal-assisted nucleophilic attack.<sup>3</sup> In particular, Eisenstein and Hoffmann proposed an elegant explanation of metal acceleration by their EH-MO approach.<sup>3b</sup> Up to the present time, however, very little has been determined on a quantitative level about metal-assisted nucleophilic attack, such as the energetics, activation barrier, and changes in geometry, electron distribution, and bonding.

In this work, ab initio MO calculations are carried out on palladium(II)-assisted nucleophilic attack on a coordinated ethylene. The palladium(II) complex is one of the most useful metal complexes in various catalytic reactions and organic syntheses,<sup>1,2</sup> such as the Wacker process, aminopalladation of olefins,<sup>4</sup> palladium-assisted alkylation of olefins,<sup>5</sup> and so on,<sup>4c,6</sup>

Chart I

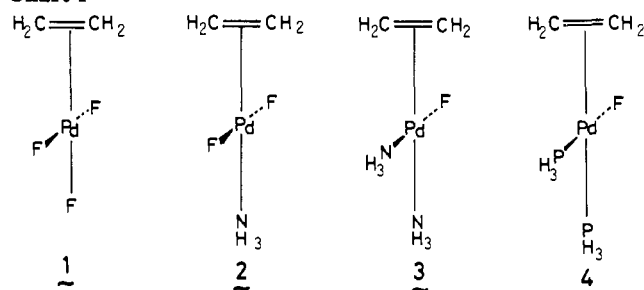
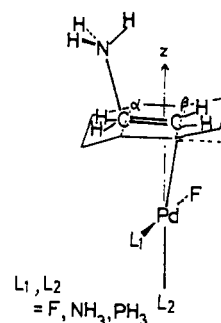


Chart II



in which nucleophilic attack on an olefin is involved as a key step. This is the reason the palladium(II) system is examined here. Of the many palladium(II)-assisted reactions, aminopalladation of olefins would appear to be the easiest for a theoretical study, because the nucleophile is a neutral amine and the reaction course (trans attack of the nucleophile) has been verified experimentally.<sup>4d,e</sup> However, several issues are still ambiguous in this reaction: first, the identity of the active species, and second, the reason for the extreme facility of this reaction. For instance, the reaction can proceed even at  $-40$  to  $-50$  °C.<sup>4b,d</sup> In this theoretical work, we hope to answer the above-mentioned questions, i.e., (a) to elucidate the mechanism of palladium acceleration and the factors contributing to the activation of olefins, (b) to clarify the nature of the active species, and (c) to estimate the activation barrier of the reaction. The emphasis, and point of departure from previous work, is on presenting a semiquantitative understanding of palladium-assisted nucleophilic attack, including changes in

- (1) The following review articles have been published concerning this issue: (a) Davies, S. G.; Green, M. L. H.; Mingos, D. M. P. *Tetrahedron* **1978**, *34*, 3047. (b) Houghton, R. P. *Metal Complexes in Organic Chemistry*; Cambridge University Press: Cambridge, England, 1979; Chapter 4. (2) (a) Hartley, F. R. *The Chemistry of Platinum and Palladium*; Applied Science: London, 1973. (b) Trost, B. M. *Tetrahedron* **1977**, *33*, 2615. (c) Kochi, J. K. *Organometallic Mechanisms and Catalysis*; Academic: New York, 1978; Chapter 5. (d) Heck, R. F. *Acc. Chem. Res.* **1979**, *12*, 146. (e) Bäckvall, J.-E. *Ibid.* **1983**, *16*, 335. (3) (a) Sakaki, S.; Nishikawa, M.; Ohyoshi, A. *J. Am. Chem. Soc.* **1980**, *102*, 4062. (b) Eisenstein, O.; Hoffmann, R. *Ibid.* **1980**, *102*, 6148; **1981**, *103*, 4308. (c) Bäckvall, J.-E.; Björkman, E. E.; Petterson, L.; Siegbahn, P. *Ibid.* **1984**, *106*, 4369; **1985**, *107*, 7265. (d) Fujimoto, H.; Yamasaki, T. *Ibid.* **1986**, *108*, 578. (e) Sakaki, S.; Maruta, K.; Ohkubo, K. *J. Chem. Soc., Dalton Trans.* **1987**, 361. (4) (a) Åkermark, B.; Bäckvall, J.-E.; Siirala-Hansén, K.; Sjöberg, K.; Zetterberg, K. *Tetrahedron Lett.* **1974**, 1363. (b) Åkermark, B.; Bäckvall, J.-E. *Ibid.* **1975**, 819. (c) Hegedus, L. S.; Siirala-Hansén, K. *J. Am. Chem. Soc.* **1975**, *97*, 1184. (d) Bäckvall, B. *Tetrahedron Lett.* **1978**, 163. (e) Bäckvall, J.-E.; Björkman, E. E. *J. Org. Chem.* **1980**, *45*, 2893. (f) Bäckvall, J.-E.; Björkman, E. E.; Byström, S. E. *Tetrahedron Lett.* **1982**, 943. (g) Bäckvall, J.-E.; Byström, S. E. *J. Org. Chem.* **1982**, *47*, 1126. (5) (a) Hayashi, T.; Hegedus, L. S. *J. Am. Chem. Soc.* **1977**, *99*, 7093. (b) Murahashi, S.; Yamamura, M.; Mita, N. *J. Org. Chem.* **1977**, *42*, 2870. (c) Hegedus, L. S.; Hayashi, T.; Darlington, W. H. *J. Am. Chem. Soc.* **1978**, *100*, 7747. (d) Kurosawa, H.; Asada, N. *Tetrahedron Lett.* **1979**, 255. (e) Hegedus, L. S.; Williams, R. E.; McGuire, M. A.; Hayashi, T. *J. Am. Chem. Soc.* **1980**, *102*, 4973.

- (6) (a) Henry, P. M. *Acc. Chem. Res.* **1973**, *6*, 16; *J. Am. Chem. Soc.* **1972**, *94*, 7305; *J. Org. Chem.* **1967**, *32*, 2575; **1973**, *38*, 1681; **1974**, *39*, 3871. (b) Still, J. K.; James, D. E.; Hines, L. F. *J. Am. Chem. Soc.* **1973**, *95*, 5062. (c) Bäckvall, J.-E. *J. Chem. Soc., Chem. Commun.* **1977**, 413. (d) Bäckvall, J. E.; Åkermark, B.; Ljunggren, S. O. *J. Am. Chem. Soc.* **1979**, *101*, 2411. (e) Kurosawa, H.; Majima, T.; Asada, N. *Ibid.* **1980**, *102*, 6996.

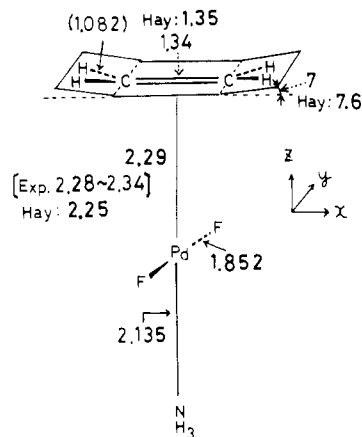


**Figure 1.** Optimized structure of  $\text{PdF}_2(\text{NH}_3)(\text{C}_2\text{H}_4)$  (bond lengths in angstroms and bond angles in degrees). Values in parentheses are assumed values taken from the optimized structure of the fragment molecule,<sup>13a</sup> the value in brackets is the experimental value of  $[\text{PdCl}_2(\text{C}_2\text{H}_4)]_2$ ,<sup>14</sup> and the values marked "Hay" are the optimized values for  $[\text{PdCl}_3(\text{C}_2\text{H}_4)]^-$  by Hay.<sup>15</sup>

total energy, geometry, and electron distribution.

### Computational Details

All-electron ab initio MO calculations were carried out on  $[\text{PdF}_3(\text{C}_2\text{H}_4)]^-$  (1),  $\text{PdF}_2(\text{NH}_3)(\text{C}_2\text{H}_4)$  (2),  $[\text{PdF}(\text{NH}_3)_2(\text{C}_2\text{H}_4)]^+$  (3), and  $[\text{PdF}(\text{PH}_3)_2(\text{C}_2\text{H}_4)]^+$  (4) (Chart I), and the reaction systems of the nucleophilic attack of  $\text{NH}_3$  on the coordinated ethylene in 1–4 (Chart II), by using the IMSPAK<sup>7</sup> and Gaussian 82<sup>8</sup> program systems. Two kinds of basis sets were employed. In the smaller basis (SB) set, MIDI-1<sup>9a</sup> and STO-3G<sup>10</sup> were used for palladium and ligand atoms, respectively, where three p-type primitives,<sup>11</sup> contracted to minimal, were added to MIDI-1 to describe the 5p orbital of palladium. With this basis set, geometry optimization was carried out. In the larger basis (LB) set, the MIDI-1 set for palladium was augmented with one diffuse Gaussian d orbital (exponent 0.11)<sup>12</sup> and then contracted to [333321/33321/3211]. For ligand atoms, the usual MIDI-1 sets were used.<sup>9b,c</sup> This LB set was employed in a discussion of energetics, bonding, and electron distribution.

Geometry optimization with parabolic fitting of total energies was carried out on some important bond distances and bond angles. For instance, the Pd—C, C=C, Pd—F, and Pd—N bond distances and the  $\text{CH}_2$  bending angles were optimized in  $\text{PdF}_2(\text{NH}_3)(\text{C}_2\text{H}_4)$ , with the remaining geometrical parameters of  $\text{C}_2\text{H}_4$  and the structure of  $\text{NH}_3$  being taken from the literature (optimized values with STO-3G set).<sup>13</sup> Those optimized values agree well with experimental<sup>14</sup> and optimized values<sup>15</sup> of similar complexes, as compared in Figure 1. In the nucleophilic attack of  $\text{NH}_3$  on  $\text{PdF}_2(\text{NH}_3)(\text{C}_2\text{H}_4)$ , the  $\text{C}^\alpha\text{—NH}_3$  distance was taken as a reaction coordinate and geometrical parameters such as the  $\text{C}^\alpha\text{—C}^\beta$  and Pd— $\text{C}^\beta$  distances, the  $\text{NC}^\alpha\text{C}^\beta$ ,  $\text{C}^\alpha\text{C}^\beta\text{Pd}$ , and  $z\text{PdC}^\beta$  angles ( $z = z$  axis), and the  $\text{C}^\alpha\text{H}_2$  and  $\text{C}^\beta\text{H}_2$  bendings were optimized independently (see Chart II for  $\text{C}^\alpha$ ,  $\text{C}^\beta$ , etc.).<sup>16</sup> These values were adopted in the other palladi-

**Table I.** Energy Decomposition Analysis (kcal/mol) of the Interaction between  $\text{C}_2\text{H}_4$  and  $\text{PdF}_n\text{L}_{3-n}$  ( $n = 1-3$ ,  $\text{L} = \text{NH}_3$  or  $\text{PH}_3$ ) and Changes in Mulliken Population Caused by the Coordination of Ethylene

	$[\text{PdF}_3(\text{C}_2\text{H}_4)]^-$	$\text{PdF}_2(\text{NH}_3)(\text{C}_2\text{H}_4)$	$[\text{PdF}(\text{NH}_3)_2(\text{C}_2\text{H}_4)]^+$	$[\text{PdF}(\text{PH}_3)_2(\text{C}_2\text{H}_4)]^+$
Energy Decomposition Analysis				
BE	-16.1	-18.0	-24.2	-23.5
DEF <sup>a</sup>	1.4	1.4	1.4	1.4
INT	-17.5	-19.4	-25.6	-24.9
ES	-45.5	-46.2	-46.2	-47.9
EX	55.7	55.0	54.8	59.3
FCTPLX	-10.8	-15.4	-20.6	-22.6
BCTPLX	-11.9	-9.4	-11.7	-11.7
R	-5.0	-3.4	-1.9	-2.0
Changes in Mulliken Population <sup>b</sup>				
Pd	+0.12	+0.23	+0.28	+0.26
$\text{C}_2\text{H}_4$	-0.11	-0.24	-0.34	-0.38
cis ligand	-0.01 (F)	0 (F)	+0.02 (F)	+0.02 (F)
trans ligand	0 (F)	+0.01 (NH <sub>3</sub> )	+0.02 (NH <sub>3</sub> )	+0.03 (PH <sub>3</sub> )

<sup>a</sup> The same geometry of  $\text{C}_2\text{H}_4$  is assumed in these complexes (see text). The structure of the  $\text{PdF}_n\text{L}_{3-n}$  fragment was taken to be the same as the structure of the corresponding part in the total complex, and the DEF value of the  $\text{PdF}_n\text{L}_{3-n}$  fragment was not considered. <sup>b</sup> "+" means an increase in Mulliken population upon the coordination of ethylene, and "-" means a decrease in Mulliken population.

um(II)-ethylene complexes and reaction systems for  $\text{NH}_3$  attack, to save CPU time, because of the large systems examined.

In an attempt to investigate in detail the coordinate bond of ethylene to palladium and the interaction between the nucleophile,  $\text{NH}_3$ , and the palladium(II)-ethylene complex, the energy decomposition analysis proposed by Morokuma et al.<sup>17</sup> was applied here. In this analysis, a total system is considered to consist of two parts; for instance, the palladium-ethylene complex is composed of the ethylene ligand and the remaining palladium part, and the reaction system of the  $\text{NH}_3$  nucleophilic attack is composed of the nucleophile,  $\text{NH}_3$ , and the palladium-ethylene complex. The binding energy (BE) is defined as stabilization of a total system, A-B, compared to separated fragments A and B taking their equilibrium structures, and it can be represented as

$$\text{BE} = E_i(\text{A-B}) - E_i(\text{A})_{\text{eq}} - E_i(\text{B})_{\text{eq}} = \text{DEF} + \text{INT}$$

$$\text{DEF} = \{E_i(\text{A})_{\text{dist}} - E_i(\text{A})_{\text{eq}}\} + \{E_i(\text{B})_{\text{dist}} - E_i(\text{B})_{\text{eq}}\}$$

$$\text{INT} = E_i(\text{AB}) - E_i(\text{A})_{\text{dist}} - E_i(\text{B})_{\text{dist}}$$

where the subscripts "eq" and "dist" mean the equilibrium and distorted structures, respectively. DEF (deformation energy) is the destabilization energy to deform A and B from their equilibrium structures to their distorted structures taken in the total system. INT (interaction energy) is the stabilization of the total system compared to the distorted fragments of A and B and is further divided into various chemically meaningful terms:

$$\text{INT} = \text{ES} + \text{EX} + \text{FCTPLX} + \text{BCTPLX} + R$$

ES and EX are the Coulombic electrostatic interaction and the exchange repulsion interaction, respectively. FCTPLX contains the charge transfer from the Lewis base, B, to the Lewis acid, A, the polarization of A, and their coupling term. BCTPLX contains the charge transfer from A to B, the polarization of B, and their coupling term, and R is the higher order remaining term. In the case of the palladium-ethylene complex, FCTPLX is defined so as to include the charge transfer from ethylene to the remaining palladium part, according to the general concept of the coordinate bond. In the reaction systems of  $\text{NH}_3$  attack, FCTPLX is defined to include the charge transfer from the nucleophile,  $\text{NH}_3$ , to the palladium-olefin complex, considering the Lewis basicity of the nucleophile,  $\text{NH}_3$ .

### Results and Discussion

**The Coordinate Bond in Palladium-Ethylene Complexes.** Before we start to discuss the nucleophilic attack of  $\text{NH}_3$  on the coord-

- Morokuma, K.; Kato, S.; Kitaura, K.; Ohmine, I.; Sakai, S.; Obara, S. IMS Computer Center Program Library; Institute for Molecular Science: Okazaki, Japan, 1980; No. 0372.
- Binkley, J. S.; Frisch, M. J.; DeFrees, D. J.; Raghavachari, K.; Whiteside, R. A.; Schlegel, H. B.; Pople, J. A. *Gaussian 82*; Carnegie-Mellon Chemistry Publishing Unit: Pittsburgh, PA, 1984.
- (a) Sakai, Y.; Tatewaki, H.; Huzinaga, S. *J. Comput. Chem.* **1982**, *3*, 6. (b) Tatewaki, H.; Huzinaga, S. *Ibid.* **1980**, *1*, 205. (c) For the hydrogen atom, the split-valence basis set proposed by Huzinaga-Dunning was used: Dunning, T. H.; Hay, P. J. In *Method of Electronic Structure Theory*; Schaeffer, H. F., Ed.; Plenum: New York, 1977.
- (a) Hehre, W. J.; Stewart, R. F.; Pople, J. A. *J. Chem. Phys.* **1969**, *51*, 2657. (b) Hehre, W. J.; Ditchfield, R.; Stewart, R. F.; Pople, J. A. *Ibid.* **1970**, *52*, 2769.
- The coefficients and exponents are taken to be the same as those of the Pd 5s orbital of the MINI-1 set.
- This value was obtained by the even-tempered criterion.
- (a) Binkley, J. S.; Pople, J. A.; Hehre, W. J. *J. Am. Chem. Soc.* **1980**, *102*, 939. Gordon, M. S.; Binkley, J. S.; Pople, J. A.; Pietro, W. J.; Hehre, W. J. *Ibid.* **1982**, *104*, 2797. (b) In  $[\text{PdF}(\text{PH}_3)_2(\text{C}_2\text{H}_4)]^+$ , the Pd— $\text{PH}_3$  distance was taken from the experimental structure of a similar complex: Ferguson, G.; McCrindle, R.; McAlees, A. J.; Parvez, M. *Acta Crystallogr., Sect. B: Struct. Crystallogr. Cryst. Chem.* **1982**, *B38*, 3679.
- Dempsey, J. N.; Baenziger, N. C. *J. Am. Chem. Soc.* **1955**, *77*, 4984.
- Hay, P. J. *J. Am. Chem. Soc.* **1981**, *103*, 1390.

- During the reaction, the Pd—F, Pd— $\text{NH}_3$ , and Pd— $\text{PH}_3$  distances were not reoptimized, considering that the Hg—ligand distance was changed little by nucleophilic attack on ethylene coordinated to Hg.<sup>36</sup>
- (a) Morokuma, K. *Acc. Chem. Res.* **1977**, *10*, 294. (b) Kitaura, K.; Morokuma, K. *Int. J. Quantum Chem.* **1976**, *10*, 325. (c) Kitaura, K.; Sakai, S.; Morokuma, K. *Inorg. Chem.* **1981**, *10*, 2292.

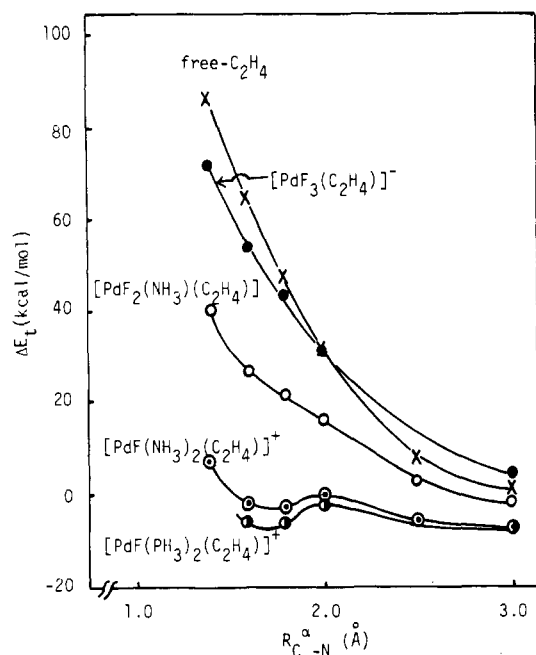


**Figure 2.** Energy change caused by the  $\text{NH}_3$  nucleophilic attack on  $\text{PdF}_n\text{L}_{3-n}(\text{C}_2\text{H}_4)$  ( $\text{L} = \text{NH}_3$  or  $\text{PH}_3$ ;  $n = 1-3$ ;  $\Delta E_i = E_i(\text{PdF}_n\text{L}_{3-n}(\text{C}_2\text{H}_4) \leftarrow \text{NH}_3) - E_i(\text{PdF}_n\text{L}_{3-n}(\text{C}_2\text{H}_4)) - E_i(\text{NH}_3)$ ).

ordinated ethylene, the coordinate bond in the palladium-ethylene complexes will be investigated, in order to obtain some useful information on the relation between the coordinate bond and the reactivity. Results of energy decomposition analysis are listed in Table I, together with changes in Mulliken population caused by the coordination of ethylene. The binding of ethylene becomes stronger in the order  $[\text{PdF}_3(\text{C}_2\text{H}_4)]^- < \text{PdF}_2(\text{NH}_3)(\text{C}_2\text{H}_4) < [\text{PdF}(\text{PH}_3)_2(\text{C}_2\text{H}_4)]^+ < [\text{PdF}(\text{NH}_3)_2(\text{C}_2\text{H}_4)]^+$ . It is noted that although the ES, EX, and BCTPLX interactions do not exhibit large changes among the complexes examined, the FCTPLX stabilization increases with increasing binding energy except for  $[\text{PdF}(\text{PH}_3)_2(\text{C}_2\text{H}_4)]^+$ . This complex suffers more from the EX repulsion than  $[\text{PdF}(\text{NH}_3)_2(\text{C}_2\text{H}_4)]^+$ , probably due to larger steric repulsion between ethylene and bulky  $\text{PH}_3$  ligands, which leads to the binding energy of this complex being slightly smaller than that of  $[\text{PdF}(\text{NH}_3)_2(\text{C}_2\text{H}_4)]^+$  despite the greater FCTPLX stabilization in the former.

Corresponding to the increasing order of the FCTPLX stabilization, the electron population of  $\text{C}_2\text{H}_4$  decreases in the order  $\text{I} > \text{II} > \text{III} > \text{IV}$ , as shown in Table I. Electron populations of other ligands exhibit interesting changes upon ethylene coordination; although the electron populations of F and  $\text{NH}_3$  are affected little by ethylene coordination, the electron population of the trans  $\text{PH}_3$  ligand is increased somewhat, indicating that ethylene coordination hardly influences electron donation from F and  $\text{NH}_3$  to Pd but weakens electron donation from trans  $\text{PH}_3$  to Pd. This difference between F,  $\text{NH}_3$ , and  $\text{PH}_3$  is suggestive of the nature of ligands. Hard ligands such as F and  $\text{NH}_3$  have a tendency to keep the strength of electron donation constant, but a soft ligand like  $\text{PH}_3$  has an ability to control the extent of electron donation from  $\text{PH}_3$  to Pd so as to keep the electron density of the central metal at the appropriate value. These features of coordinate bond and ligand character will be discussed later in relation to the palladium acceleration of nucleophilic attack.

**Changes in Total Energy and Geometry during  $\text{NH}_3$  Attack.** Changes in the total energy,  $\Delta E_i$ , of the reaction system  $[\text{PdF}_n\text{L}_{3-n}(\text{C}_2\text{H}_4)] \leftarrow \text{NH}_3$  ( $n = 1-3$ ;  $\text{L} = \text{NH}_3$  or  $\text{PH}_3$ ) are given as a function of the  $\text{C}^\alpha\text{-N}$  distance in Figure 2, where a standard (zero energy) is taken for  $R_{\text{C}^\alpha\text{-N}} = \infty$ . Approach of the nucleophile,  $\text{NH}_3$ , to free  $\text{C}_2\text{H}_4$ ,  $[\text{PdF}_3(\text{C}_2\text{H}_4)]^-$ , and  $\text{PdF}_2(\text{NH}_3)(\text{C}_2\text{H}_4)$  yields substantial destabilization. On the other hand, attack of  $\text{NH}_3$  on  $[\text{PdF}(\text{NH}_3)_2(\text{C}_2\text{H}_4)]^+$  and  $[\text{PdF}(\text{PH}_3)_2(\text{C}_2\text{H}_4)]^+$  proceeds very easily with activation barriers of ca. 8 and 6 kcal/mol,<sup>18a,b</sup> respectively. These values, of course, must be

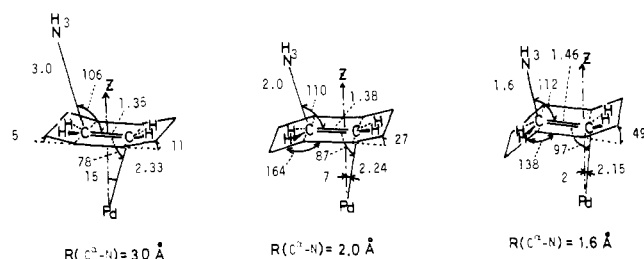


**Figure 3.** Geometry change of the palladium-ethylene moiety along the reaction coordinate for nucleophilic addition of  $\text{NH}_3$  to the coordinated ethylene (bond lengths in angstroms and bond angles in degrees). Ligand parts are omitted, because those positions are fixed during the reaction.

corrected by introducing electron correlation effects and basis set superposition error (BSSE), which will be briefly discussed later. Even though these activation energies should be corrected, the above results suggest that a cationic palladium(II)-olefin complex is an active species of this reaction.<sup>18c,d</sup> In fact, the palladium-assisted alkylation and amination of olefins are accelerated very much by addition of excess amine, which should form a cationic palladium complex.<sup>4c,d,f,5a,c-e</sup> Furthermore, Kurosawa and his collaborators have reported that the facile attack of nucleophiles on the coordinated olefins occurs in isolated cationic palladium(II) complexes.<sup>5d,6e</sup> These experimental results are consistent with our suggestion that the active species is a cationic palladium(II)-olefin complex.

The geometry change of the palladium-ethylene complex along the reaction coordinate ( $R_{\text{C}^\alpha\text{-N}}$ ) is displayed in Figure 3. Several interesting features are found; when  $\text{NH}_3$  approaches  $\text{C}_2\text{H}_4$ , the  $\text{C}^\alpha\text{-C}^\beta$  and  $\text{Pd-C}^\alpha$  bond distances are lengthened, the  $\text{Pd-C}^\beta$  distance is shortened, and simultaneously the  $\text{C}^\alpha\text{H}_2$  and  $\text{C}^\beta\text{H}_2$  bendings are increased. These changes in geometry correspond with the conversions of the  $\text{C}^\alpha=\text{C}^\beta$  double bond to the  $\text{C}^\alpha\text{-C}^\beta$  single bond and of the  $\eta^2$ -coordinated ethylene to the  $\eta^1$ -coordinated alkyl group. Another interesting feature is that these geometrical changes arise simultaneously and smoothly, suggesting that the bond formation and bond breaking occur in a concerted manner.

Near the transition state (at  $R_{\text{C}^\alpha\text{-N}} = 2.0 \text{ \AA}$ ), the  $\text{C}^\alpha\text{-C}^\beta$  distance lengthens by only  $0.04 \text{ \AA}$ , about 20% of the total increase, if the  $\text{C}^\alpha\text{-C}^\beta$  distance of the product is taken as  $1.54 \text{ \AA}$  (the standard value for the  $\text{C-C}$  single bond).<sup>19</sup> The  $\text{C}^\alpha\text{H}_2$  and  $\text{C}^\beta\text{H}_2$  bendings increase by about  $20^\circ$  at  $R_{\text{C}^\alpha\text{-N}} = 2.0 \text{ \AA}$ , which corresponds to about 40% of the total increase in the  $\text{CH}_2$  bending, if the product is assumed to have tetrahedral bond angles around the  $\text{C}^\alpha$  and  $\text{C}^\beta$  atoms. These geometrical changes indicate a signal that the transition state is not late but rather early, which will be also supported by the other results, as discussed later.

**Changes in Electron Distribution during the Reaction.** Changes in the Mulliken population caused by  $\text{NH}_3$  attack are given in Figure 4, as a function of the reaction coordinate. Approach of  $\text{NH}_3$  to ethylene significantly decreases the electron population of  $\text{NH}_3$  and substantially increases the electron population of the

(18) (a) These values correspond to the destabilization in total energy relative to that of  $R_{\text{C}^\alpha\text{-N}} = 3.0 \text{ \AA}$ . Although this estimation of the activation barrier is not correct, strictly speaking, the value estimated does not seem unreasonable, because both structures at  $R_{\text{C}^\alpha\text{-N}} = 3.0$  and  $2.5 \text{ \AA}$  exhibit almost the same  $E_i$  value in  $[\text{PdF}(\text{NH}_3)_2(\text{C}_2\text{H}_4)]^+$ . (b) The products obtained from  $[\text{PdF}(\text{NH}_3)_2(\text{C}_2\text{H}_4)]^+$  and  $[\text{PdF}(\text{PH}_3)_2(\text{C}_2\text{H}_4)]^+$  are less stable than the reactants at  $R_{\text{C}^\alpha\text{-N}} = 3.0 \text{ \AA}$ . This rather unreasonable feature might arise from the neglect of the electron correlation effect and solvation effect, no optimization of the  $\text{N-H}$  bond length, etc. (c) Introducing an electron correlation energy with the MP2 method stabilizes the product relative to the reactant; for the model system  $[\text{PdF}(\text{C}_2\text{H}_4)] \leftarrow \text{NH}_3$ ,  $\Delta E_{\text{corr}} = E_{\text{corr}}(R_{\text{C}^\alpha\text{-N}} = 1.6 \text{ \AA}) - E_{\text{corr}}(R_{\text{C}^\alpha\text{-N}} = 3.0 \text{ \AA}) = -7.0 \text{ kcal/mol}$ . Even if this value is taken into consideration for  $[\text{PdF}_3(\text{C}_2\text{H}_4)] \leftarrow \text{NH}_3$  and  $\text{PdF}_2(\text{NH}_3)(\text{C}_2\text{H}_4) \leftarrow \text{NH}_3$ , effective stabilization cannot be expected at their product sides. (d) When the reactivities of cationic, neutral, and anionic palladium(II)-olefin complexes with a polar reagent are compared, differences in BSSE, solvation effect, electron correlation, and so on must be taken into consideration. Some of them are being investigated now.

(19) Sutton, L. E., Ed. *Spec. Publ.—Chem. Soc.* 1965, No. 18.

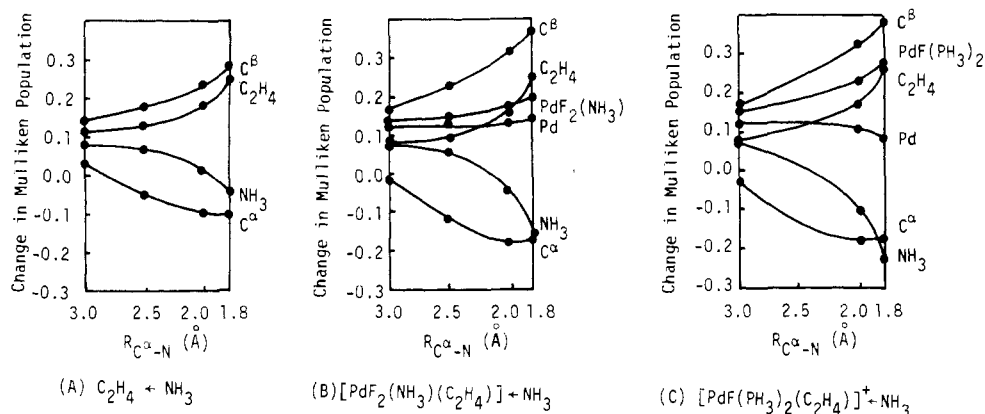


**Figure 4.** Changes in Mulliken population (change =  $\rho(\text{Pd-ethylene} \leftarrow \text{NH}_3) - \rho(\text{Pd-ethylene}) - \rho(\text{NH}_3)$ ) along the reaction coordinate for nucleophilic addition of  $\text{NH}_3$  to the coordinated ethylene.

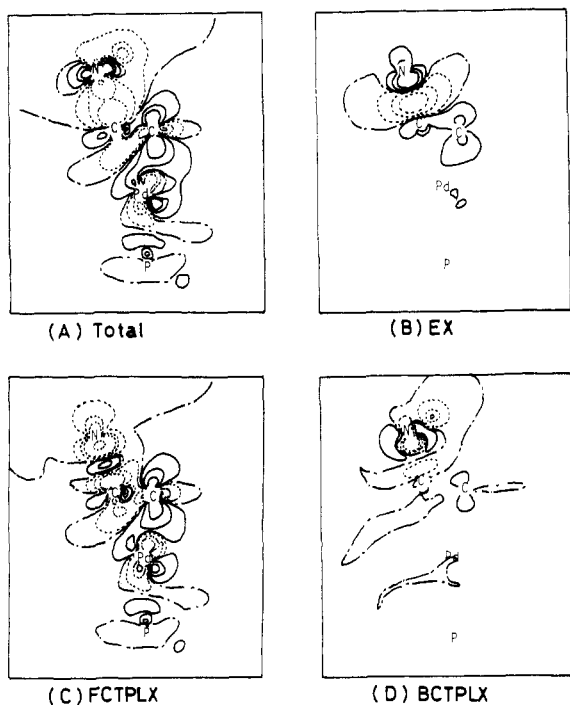
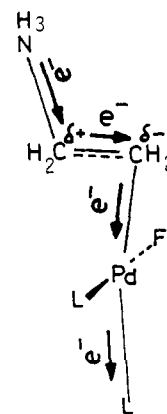


**Figure 5.** Difference density maps of the reaction system  $[\text{PdF}(\text{PH}_3)_2(\text{C}_2\text{H}_4)]^+ + \text{NH}_3$  (difference =  $\rho([\text{PdF}(\text{PH}_3)_2(\text{C}_2\text{H}_4)]^+ \leftarrow \text{NH}_3) - \rho([\text{PdF}(\text{PH}_3)_2(\text{C}_2\text{H}_4)]^+) - \rho(\text{NH}_3)$ ): (—) increase in the density of 0.001, 0.005, 0.01, and 0.05; (---) decrease in the density of -0.001, -0.005, -0.01, and -0.05; (- - -) 0.0.

$\text{C}_2\text{H}_4$  moiety, suggesting the importance of the charge transfer from  $\text{NH}_3$  to  $\text{C}_2\text{H}_4$ . In spite of this significant charge transfer from  $\text{NH}_3$  to  $\text{C}_2\text{H}_4$ , the transferred electrons from  $\text{NH}_3$  do not distribute uniformly over the  $\text{C}_2\text{H}_4$  moiety but accumulate on the  $\text{C}^\beta$  atom, as shown by the considerable increase of the  $\text{C}^\beta$  atomic population and the remarkable decrease of the  $\text{C}^\alpha$  atomic population (see Figure 4). These changes imply that not only the simple charge transfer from  $\text{NH}_3$  to  $\text{C}_2\text{H}_4$  but also polarization of the  $\text{C}_2\text{H}_4$  moiety takes place in the reaction. Approach of  $\text{NH}_3$  to  $\text{C}_2\text{H}_4$  also gradually increases the electron population of the  $\text{PdF}_n\text{L}_{3-n}$  group (Figure 4), which means that the charge transfer from  $\text{C}_2\text{H}_4$  to  $\text{PdF}_n\text{L}_{3-n}$  simultaneously occurs. However, the atomic population of palladium hardly increases, especially in the case of  $[\text{PdF}(\text{PH}_3)_2(\text{C}_2\text{H}_4)]^+$ . Again, this result cannot be explained by the simple charge transfer from  $\text{C}_2\text{H}_4$  to  $\text{PdF}_n\text{L}_{3-n}$  but by the polarization of  $\text{PdF}_n\text{L}_{3-n}$  coupled with the charge transfer from  $\text{C}_2\text{H}_4$  to  $\text{PdF}_n\text{L}_{3-n}$ .

The above-described changes in electron distribution are represented more clearly by the difference density map of Figure 5A, in which the difference density of the  $[\text{PdF}(\text{PH}_3)_2(\text{C}_2\text{H}_4)]^+ \leftarrow \text{NH}_3$  system is given as a typical example. Electron density decreases in the region of the lone-pair orbital of  $\text{NH}_3$ , which is in accordance

**Chart III**



with the charge transfer from  $\text{NH}_3$  to  $\text{C}_2\text{H}_4$ . In the  $\text{C}_2\text{H}_4$  moiety, electron density decreases near the  $\text{C}^\alpha$  atom but increases near the  $\text{C}^\beta$  atom, indicating the polarization of this moiety. Near the Pd atom, however, complicated changes of electron distribution are found; the electron density decreases in the region pointing to the  $\text{C}^\beta$  atom, probably because the electron density of the  $d_\sigma$  orbital might be reduced so as to weaken the EX repulsion with the accumulated electron density on the  $\text{C}^\beta$  atom. In the other region around the Pd atom, the electron density is increased, due to the charge transfer from  $\text{C}^\beta$  to Pd. Also, a very small but nonnegligible increase of the electron density is found at the region of the lone pair of the trans ligand. These features found in the difference density map suggest that the nucleophilic attack causes both simple charge transfer from  $\text{C}_2\text{H}_4$  to Pd and polarization of  $\text{PdF}_n\text{L}_{3-n}$ . In summary, four kinds of redistribution of electrons arise from the nucleophilic attack, as schematically depicted in Chart III; the first is the charge transfer from  $\text{NH}_3$  to  $\text{C}_2\text{H}_4$ , the second is the polarization of  $\text{C}_2\text{H}_4$ , the third is the charge transfer from  $\text{C}_2\text{H}_4$  to  $\text{PdF}_n\text{L}_{3-n}$ , and the last is the polarization of  $\text{PdF}_n\text{L}_{3-n}$ .

Changes in electron distribution will now be compared among the reaction systems examined. As shown in Figure 6, the electron population of the nucleophile,  $\text{NH}_3$ , decreases with increasing reactivity of the complex, i.e.,  $[\text{PdF}_3(\text{C}_2\text{H}_4)]^- > \text{PdF}_2(\text{NH}_3)(\text{C}_2\text{H}_4) > [\text{PdF}(\text{NH}_3)_2(\text{C}_2\text{H}_4)]^+ > [\text{PdF}(\text{PH}_3)_2(\text{C}_2\text{H}_4)]^+$ , indicating the importance of charge transfer from  $\text{NH}_3$  to  $\text{C}_2\text{H}_4$ . The electron population of the  $\text{PdF}_n\text{L}_{3-n}$  group also increases linearly with increasing reactivity, whereas electron populations of both  $\text{C}_2\text{H}_4$  and Pd increase in the order  $[\text{PdF}_3(\text{C}_2\text{H}_4)]^- < \text{PdF}_2(\text{NH}_3)(\text{C}_2\text{H}_4) < [\text{PdF}(\text{NH}_3)_2(\text{C}_2\text{H}_4)]^+ < [\text{PdF}(\text{PH}_3)_2(\text{C}_2\text{H}_4)]^+$ . From these results, it is considered important to the acceleration of nucleophilic attack that the  $\text{PdF}_n\text{L}_{3-n}$  group has enough ability to accept charge transfer from  $\text{C}_2\text{H}_4$ . The reason for the importance of this charge transfer is unambiguous; the greater ability of the  $\text{PdF}_n\text{L}_{3-n}$  group to accept electrons results in smaller electron population of the  $\text{C}_2\text{H}_4$  moiety, which strengthens charge transfer from the nucleophile,  $\text{NH}_3$ , to  $\text{C}_2\text{H}_4$ .

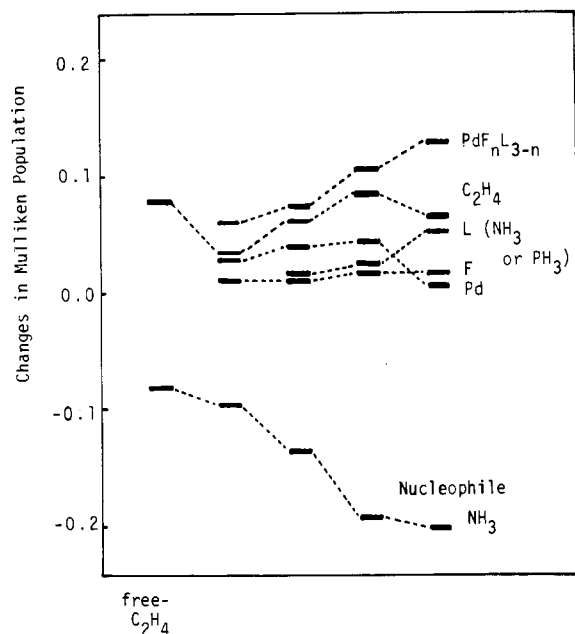


**Figure 6.** Changes in Mulliken population near the transition state ( $R_{C\alpha-N} = 2.0 \text{ \AA}$ ; change =  $\rho(\text{Pd-ethylene} \leftarrow \text{NH}_3) - \rho(\text{Pd-ethylene}) - \rho(\text{NH}_3)$ ).

**Table II.** Energy Decomposition Analysis (kcal/mol) of the Interaction between the Nucleophile  $\text{NH}_3$  and the Palladium-Ethylene Complex

	free- $\text{C}_2\text{H}_4$	$[\text{PdF}_3^- (\text{C}_2\text{H}_4)]^-$	$[\text{PdF}(\text{NH}_3)_2 (\text{C}_2\text{H}_4)]^+$	$[\text{PdF}(\text{PH}_3)_2 (\text{C}_2\text{H}_4)]^+$
$R_{C\alpha-N} = 3.0 \text{ \AA}$				
INT	0.6	3.2 (+2.6) <sup>a</sup>	-8.1 (-8.7) <sup>a</sup>	-8.5 (-9.1) <sup>a</sup>
ES	0.5	3.0 (+2.5)	-6.7 (-7.2)	-6.9 (-7.4)
EX	2.5	2.6 (+0.1)	2.2 (-0.3)	2.2 (-0.3)
FCTPLX	-2.2	-2.1 (+0.1)	-3.2 (-1.0)	-3.2 (-1.0)
BCTPLX	-0.2	-0.3 (-0.1)	-0.3 (-0.1)	-0.3 (0)
R	0	0	-0.1 (-0.1)	-0.3 (-0.3)
$R_{C\alpha-N} = 2.0 \text{ \AA}$				
INT	28.2	21.9 (-6.3)	-6.5 (-34.7)	-8.5 (-36.7)
ES	-36.0	-34.4 (+1.6)	-45.8 (-9.8)	-46.2 (-10.2)
EX	87.1	81.3 (-5.8)	71.6 (-15.5)	71.1 (-16.0)
FCTPLX	-18.8	-20.7 (-1.9)	-26.6 (-7.8)	-27.6 (-8.8)
BCTPLX	-6.3	-6.0 (+0.3)	-5.1 (+1.2)	-5.6 (+1.3)
R	2.2	1.7 (-0.5)	-0.6 (-2.8)	-0.8 (-3.0)

<sup>a</sup> The difference from the interaction of free  $\text{C}_2\text{H}_4$  with  $\text{NH}_3$  is given in parentheses.

In  $[\text{PdF}(\text{PH}_3)_2(\text{C}_2\text{H}_4)]^+$ , the atomic population of palladium only slightly increases in spite of the large increase in the electron population of the  $\text{PdF}(\text{PH}_3)_2$  group, while the atomic population of palladium increases more in the other complexes than in the  $\text{PH}_3$  analogue. This difference between the  $\text{PH}_3$  complex and the others can be easily interpreted in terms of softness of  $\text{PH}_3$ ; the  $\text{PH}_3$  ligand has an ability to keep the Pd atomic population constant by controlling electron donation from  $\text{PH}_3$  (vide supra), which would lead to the charge transfer from  $\text{C}_2\text{H}_4$  to Pd in the  $\text{PH}_3$  complex being greater than in the other complexes. The above discussion suggests that a neutral and soft ligand is desirable for the acceleration of nucleophilic attack.

**Energy Decomposition Analysis between the Nucleophile ( $\text{NH}_3$ ) and the Palladium-Ethylene Complex.** For some typical reaction systems, the interaction between the nucleophile and palladium-ethylene complexes was investigated with an energy decomposition analysis (EDA). As listed in Table II, the ES interaction is essential for the greater stabilization of the cationic palladium-ethylene systems at  $R_{C\alpha-N} = 3.0 \text{ \AA}$ , which seems reasonable because the electrostatic interaction is generally important to long-range interaction. At  $R_{C\alpha-N} = 2.0 \text{ \AA}$ , the ES, EX, and FCTPLX interactions become considerably stronger, while the increases in the BCTPLX and R stabilizations are very small.

**Table III.** Changes in Mulliken Population Caused by the  $\text{NH}_3$  Attack on  $[\text{PdF}(\text{PH}_3)_2(\text{C}_2\text{H}_4)]^{\pm a}$

	total	EX	FCTPLX	BCTPLX	R
$\text{PdF}(\text{PH}_3)_2^+$	+0.142	+0.012	+0.123	+0.004	+0.003
Pd	+0.003	+0.008	-0.002	+0.003	-0.006
F	+0.016	+0.001	+0.014	0	+0.001
cis $\text{PH}_3$	+0.055	+0.001	+0.050	0	+0.004
trans $\text{PH}_3$	+0.068	+0.002	+0.061	+0.001	+0.004
$\text{C}_2\text{H}_4$	+0.057	-0.012	+0.025	+0.015	+0.029
$\text{C}^\alpha$	-0.134	-0.057	-0.133	-0.001	+0.057
$\text{C}^\beta$	+0.077	+0.035	+0.050	+0.013	-0.021
$\text{NH}_3$	-0.199	0.0	-0.147	-0.018	-0.034

<sup>a</sup> The analysis is according to the EDA scheme ( $R_{C\alpha-N} = 2.0 \text{ \AA}$ ). “+” means an increase in Mulliken population upon the nucleophilic attack of  $\text{NH}_3$ , and “-” means a decrease.

Furthermore, the ES, EX, and FCTPLX interactions exhibit critical differences among the cationic palladium-ethylene complexes, the anionic complex, and free  $\text{C}_2\text{H}_4$ ; the cationic palladium-ethylene complexes can receive significantly larger stabilization from the ES and FCTPLX terms than the free  $\text{C}_2\text{H}_4$  and the anionic complex. On the other hand, the cationic complexes suffer less from the EX repulsion than the free  $\text{C}_2\text{H}_4$  and the anionic complex. Thus, the large acceleration of nucleophilic attack by the cationic complexes is attributed to the large stabilization from ES and FCTPLX terms and the small destabilization from the EX term. This implies that the palladium-assisted nucleophilic attack might be characterized as a frontier- and simultaneously charge-controlled reaction.

Mulliken populations (Table III) and difference density maps (Figure 5) are also analyzed according to the EDA scheme, to investigate how each interaction contributes to electron distribution. As shown in Table III and Figure 5, changes in electron distribution caused by the reaction primarily result from the FCTPLX interaction and to a lesser extent from the EX repulsion. Certainly, the total difference density map can be almost reproduced by a sum of difference density maps of EX and FCTPLX, as shown in Figure 5. These imply that FCTPLX and EX interactions are important from the point of view of the electron distribution. The greater importance of FCTPLX is also indicated by the following results: (1) The FCTPLX term decreases the electron population of  $\text{NH}_3$  but increases electron populations of both the  $\text{C}_2\text{H}_4$  moiety and the  $\text{PdF}_n\text{L}_{3-n}$  group. Simultaneously, the electron density decreases near the  $\text{C}^\alpha$  atom and increases near the  $\text{C}^\beta$  atom through this term. These changes are consistent with the overall changes of the electron distribution. (2) The difference in electron distribution between  $[\text{PdF}_3(\text{C}_2\text{H}_4)]^-$  and  $[\text{PdF}(\text{PH}_3)_2(\text{C}_2\text{H}_4)]^+$  mostly comes from the FCTPLX term (see Table III). (3) Only this term accumulates the electron density between the  $\text{C}^\alpha$  atom and the nucleophile, which corresponds to the formation of a covalent bond between the  $\text{C}^\alpha$  atom and nucleophile (see Figure 5C).

The difference density maps of Figure 5 also shed some light on the nature of the transition state. The EX interaction decreases the electron density in the region between the  $\text{C}^\alpha$  atom and the nucleophile to a greater extent than the FCTPLX interaction increases it (Figure 5B, C). This leads to a net decrease in the electron density between the  $\text{C}^\alpha$  atom and the nucleophile, as shown by the total density map of Figure 5A. In other words, the  $\text{C}^\alpha\text{-N}$  bond is not formed effectively near the transition state and the EX repulsion is still strong there. These observations are in accordance with the early transition state of the reaction (vide supra).

**Orbital Mixing near the HOMO and LUMO.** The above-described changes in electron distribution and the ligand effect on the reactivity are easily explained in terms of the orbital mixing near the HOMO and LUMO,<sup>20</sup> which arises from a second-order perturbation among the lone pair of the nucleophile ( $\phi_l$ ) and the

(20) (a) Similar orbital mixing has been proposed for the organic reactions<sup>20b</sup> and the reactions of non transition metals.<sup>3c</sup> (b) Bach, R. D.; Wolber, G. *J. Am. Chem. Soc.* **1984**, *106*, 1401.

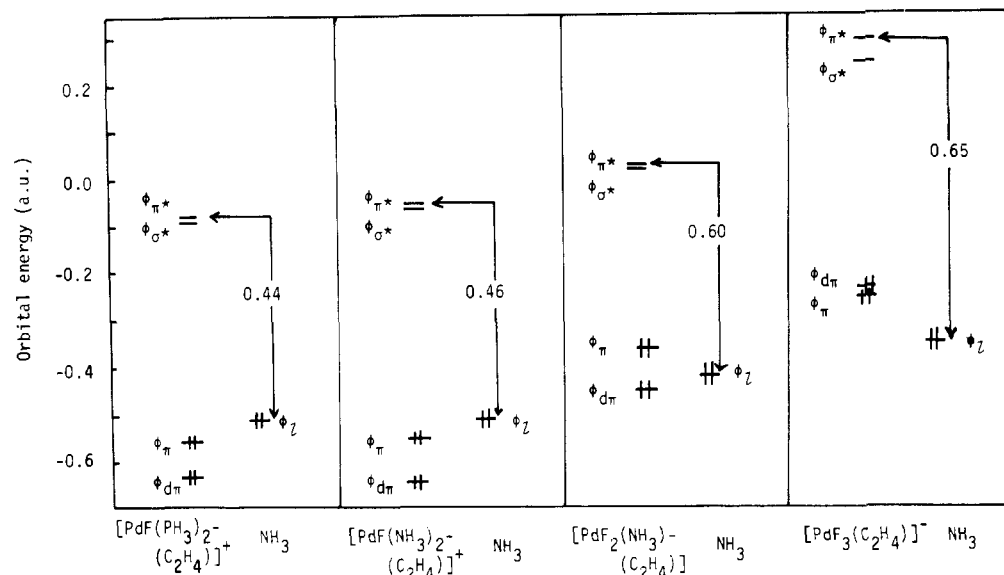


Figure 7. Energy levels of some important orbitals near the HOMO and LUMO of  $\text{PdF}_n\text{L}_{3-n}(\text{C}_2\text{H}_4)$  and  $\text{NH}_3$  ( $R_{\text{C}^\alpha-\text{N}} = 3.0 \text{ \AA}$ ).

two pairs of bonding and antibonding molecular orbitals ( $\phi_\pi$ ,  $\phi_{d\pi}$ ,  $\phi_\pi^*$ ,  $\phi_\sigma^*$ ) in the palladium–ethylene complex (see Figure 8 for these orbitals<sup>21a</sup>).

The energy levels of these orbitals are compared at  $R_{\text{C}^\alpha-\text{N}} = 3.0 \text{ \AA}$  (Figure 7). At this distance the nucleophile is considered to be under the influence of the charge in the palladium–ethylene complex but does not effectively form a covalent interaction with the  $\text{C}_2\text{H}_4$  part. The critical difference in the reaction systems is found with the relative energy levels of the lone pair of  $\text{NH}_3$  and the  $\phi_\pi$ ,  $\phi_{d\pi}$ ,  $\phi_\pi^*$ ,  $\phi_\sigma^*$  orbitals of palladium–ethylene complexes. In the cationic complexes, the energy level of the lone-pair orbital lies between those of  $\phi_\pi$  and  $\phi_\sigma^*$  orbitals, in the neutral complex lower than those of  $\phi_\pi$  and  $\phi_{d\pi}$  orbitals, and in the anionic complex lower than those of two occupied orbitals,  $\phi_\pi$  and  $\phi_{d\pi}$ .

This difference in the relative position of the lone pair leads to significantly different orbital mixings, as schematically represented in Figure 8.<sup>21b</sup> In the cationic complex, the  $\phi_1$  orbital is mainly composed of the  $\phi_{d\pi}$  orbital, into which  $\phi_l$  mixes in a bonding way. The  $\phi_\pi$ ,  $\phi_\sigma^*$ , and  $\phi_\pi^*$  orbitals also mix into this orbital, but the extent of their mixings is rather small, because their mixings are caused by the second-order term of perturbation. The  $\phi_2$  orbital mainly consists of the bonding interaction between  $\phi_l$  and  $\phi_\pi$  orbitals. The mixings of  $\phi_{d\pi}$  and  $\phi_\sigma^*$  into this orbital are small, since they arise again from the second-order term through the small overlaps of the  $\phi_l - \phi_\sigma^*$  and  $\phi_l - \phi_{d\pi}$  orbital pairs (note a small  $p_\pi$  lobe of the carbon atom in the  $\phi_{d\pi}$  and  $\phi_\sigma^*$  orbitals). The  $\phi_\pi^*$  orbital also mixes into the  $\phi_2$  orbital only a slight amount, since this mixing is caused by the second-order term and  $\phi_\pi^*$  lies much higher in energy than the  $\phi_\pi$  orbital. Thus,  $\phi_2$  is only slightly perturbed by these mixings, as schematically

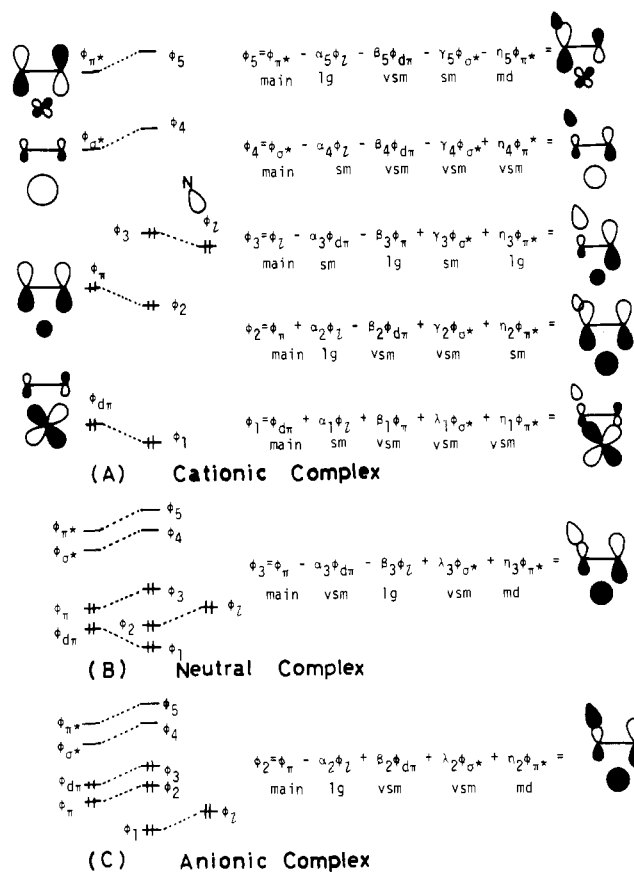


Figure 8. Schematic pictures of orbital mixing caused by the nucleophile.

depicted in Figure 8. The  $\phi_3$  orbital mainly consists of  $\phi_l - \phi_\pi$  antibonding and  $\phi_l + \phi_\pi^*$  bonding, in which the  $\phi_\pi^*$  mixing occurs with the same phase as the  $\text{C}^\beta p_\pi$  lobe of  $\phi_\pi$  but with the phase opposite to the  $\text{C}^\alpha p_\pi$  lobe of  $\phi_\pi$ . Mixings of the other orbitals,  $\phi_{d\pi}$  and  $\phi_\sigma^*$ , are rather small because of their small overlaps with  $\phi_l$  (vide supra). As a result, the  $\phi_3$  orbital is deformed as follows: the  $\text{C}^\beta p_\pi$  lobe becomes large but the  $\text{C}^\alpha p_\pi$  lobe becomes small, which strengthens the bonding interaction between Pd and  $\text{C}^\beta$  atoms and weakens bonding between Pd and  $\text{C}^\alpha$  atoms. These changes in electron distribution and bonding agree well with their overall changes described above, and any of the other orbital mixings in the  $\phi_1$  and  $\phi_2$  orbitals do not cause such changes. Of the  $\phi_l + \phi_\pi^*$  and  $\phi_l - \phi_\pi$  orbital mixings involved in  $\phi_3$ , the former mixing is more important to the reaction than the latter, because

(21) (a) The coordinate bond of ethylene to palladium is primarily contributed by the  $\sigma$ -donative interaction and secondarily by the  $\pi$  back-donation.<sup>22</sup> Thus, the  $\phi_{d\pi}$  orbital is considered to be predominantly palladium 4d in character, and  $\phi_\pi^*$  is predominantly  $\pi^*$  orbital in character, as depicted in Figure 8. (b) The orbital mixing of this work is based on the second-order perturbation, as in the orbital mixing of ref 3b. According to our orbital mixing, the  $\text{C}^\beta p_\pi$  orbital is enlarged but the  $\text{C}^\alpha p_\pi$  orbital is decreased in the occupied level. This means that in the virtual space the  $\text{C}^\beta p_\pi$  orbital is decreased and the  $\text{C}^\alpha p_\pi$  orbital is enlarged. Such changes found in the virtual space are essentially the same as those obtained in the orbital mixing of ref 3b. However, there are several differences between ref 3b and this work: (1) The orbital mixing is induced by the lone-pair orbital of the nucleophile,  $\text{NH}_3$ , in our case but by the displacement of olefin from a symmetrical ( $\eta^2$ ) coordinating position to an unsymmetrical ( $\eta^1$ -like) coordinating position in ref 3b. (2) Changes in occupied orbitals are examined in detail here, which clarifies why and how electron distribution and bonding nature change by the nucleophilic attack of  $\text{NH}_3$  on the coordinated olefin. In ref 3b, the LUMO of metal–olefin complexes is examined very well, which facilitates the prediction of the reactivity of coordinated olefin from the point of view of frontier orbital theory.

the  $\phi_l + \phi_{\pi^*}$  mixing is bonding between the  $C^\alpha$  atom and nucleophile. The acceleration by  $[\text{PdF}(\text{PH}_3)_2(\text{C}_2\text{H}_4)]^+$  being higher than that by the  $\text{NH}_3$  analogue can be explained in terms of this orbital mixing. The  $\text{PH}_3$  complex exhibits a difference in energy between the  $\phi_{\pi^*}$  and  $\phi_l$  orbitals smaller than that of the  $\text{NH}_3$  analogue by ca. 0.02 eV (see Figure 7), yielding greater mixing of the  $\phi_{\pi^*}$  orbital into the  $\phi_3$  orbital. Thus, the  $\text{PH}_3$  complex can form a stronger bonding interaction between the nucleophile and the  $C^\alpha$  atom.

In the neutral complex, the  $\phi_3$  orbital, shown in Figure 8B, is also important. Unfortunately, however, the difference in energy between  $\phi_l$  and  $\phi_{\pi^*}$  is 0.60 eV, greater than that of the cationic complex by ca. 0.15 eV, as shown in Figure 7. In the anionic complex, on the other hand, the  $\phi_2$  orbital becomes important to the reaction as shown in Figure 8C (note that the  $\phi_l$  orbital lies lower in energy than the  $\phi_{d\pi}$  and  $\phi_{\pi^*}$  orbitals, unlike the case for the neutral and the cationic complexes). Also in  $\phi_2$ , the  $\phi_l + \phi_{\pi^*}$  mixing is included as an important component. Nevertheless, the difference in energy between the  $\phi_l$  and  $\phi_{\pi^*}$  orbitals is the greatest (0.65 eV; see Figure 7), and therefore, not only the bonding mixing of  $\phi_l + \phi_{\pi^*}$  but also the deformation of the  $\phi_2$  orbital leading to the product is the smallest in the palladium-olefin complexes examined.

The relationship between results of the EDA and orbital mixing is also interesting. If the energy difference between  $\phi_{\pi^*}$  and  $\phi_l$  is small, the  $\phi_{\pi^*} + \phi_l$  mixing becomes large and thereby the strong charge transfer from  $\text{NH}_3$  to  $\text{C}_2\text{H}_4$  arises, and vice versa. This charge-transfer interaction is a main part of the FCTPLX term. Because the  $\phi_{\pi^*} + \phi_l$  mixing in  $\phi_3$  reduces the size of the  $C^\alpha$   $p_\pi$  lobe but enlarges the size of the  $C^\beta$   $p_\pi$  lobe (see Figure 8), this mixing corresponds to the polarization of the  $\text{C}_2\text{H}_4$  moiety, which is also a part of FCTPLX. The decrease in the  $C^\alpha$   $p_\pi$  lobe weakens the EX repulsion between the nucleophile and the  $C^\alpha$  atom and simultaneously strengthens the ES interaction between them. In the cationic complexes, especially in  $[\text{PdF}(\text{PH}_3)_2(\text{C}_2\text{H}_4)]^+$ , the difference in energy between  $\phi_{\pi^*}$  and  $\phi_l$  is the smallest, yielding the greatest mixing of  $\phi_{\pi^*} + \phi_l$ , the greatest stabilization from FCTPLX and ES terms, and the smallest destabilization from the EX term. In both neutral and anionic complexes, the difference in energy is rather large, which leads to smaller stabilization from the FCTPLX and ES terms and larger destabilization from the EX term.

**Ligand Effect on the Reactivity.** These results are suggestive for the ligand that facilitates metal-assisted nucleophilic attack. From the point of view of the EX and FCTPLX interactions, the metal and ligand that stabilize  $\phi_{\pi^*}$  are desirable, since the smaller difference in energy between  $\phi_l$  and  $\phi_{\pi^*}$  orbitals leads to greater orbital mixing of  $\phi_{\pi^*}$ . The  $\phi_{\pi^*}$  orbital involves an antibonding interaction between the palladium  $d\pi$  and  $\text{C}_2\text{H}_4$   $\pi^*$  orbitals, and therefore, a weak back-donative interaction between the palladium  $d\pi$  and  $\text{C}_2\text{H}_4$   $\pi^*$  orbitals results in  $\phi_{\pi^*}$  lying lower in energy. Palladium(II) complexes have been experimentally shown to exhibit a slight ability to form a  $\pi$ -back-donative interaction.<sup>22</sup> The present MO calculations also indicate that the back-donative interaction is weaker than the donative interaction except for  $[\text{PdF}_3(\text{C}_2\text{H}_4)]^-$  (see Table I).

Not only the metal but also the ligand influences the energy of the  $\phi_{\pi^*}$  orbital. As clearly shown in Figure 7, an anionic ligand pushes up the  $\phi_{\pi^*}$  orbital via electrostatic repulsion. Thus, an anionic ligand disfavors the metal-assisted nucleophilic attack.

From the point of view of charge control the ES interaction is important. As discussed in Table I, the FCTPLX interaction from  $\text{C}_2\text{H}_4$  to Pd is the weakest in  $[\text{PdF}_3(\text{C}_2\text{H}_4)]^-$ , probably owing to the high-lying acceptor orbital of palladium pushed up by electrostatic repulsion from the anionic  $\text{F}^-$  ligand. In the case of

a neutral soft ligand, such as  $\text{PH}_3$ , the electron donation from  $\text{C}_2\text{H}_4$  to Pd is the greatest, making the ethylene ligand the most positively charged and thereby yielding the greatest stabilization of the ES interaction.

**Basis Set Superposition Error (BSSE) and Electron Correlation Effects.** The corrections for BSSE<sup>23</sup> and electron correlation effects are briefly examined for a simple model system,  $[\text{PdF}(\text{C}_2\text{H}_4)]^- \leftarrow \text{NH}_3$ . Electron correlation, estimated with the MP2 method,<sup>24</sup> stabilizes the transition state by about 8 kcal/mol, compared to the structure at  $R_{\text{C}^\alpha-\text{N}} = 3.0$  Å. On the other hand, the BSSE value at the transition state was estimated to be larger than that at  $R_{\text{C}^\alpha-\text{N}} = 3.0$  Å by about 5 kcal/mol.<sup>25</sup> Because of the large size of the reaction system, a polarization function on the N atom of the nucleophile was not included in the basis set. The effect of the polarization function<sup>9b</sup> was also investigated in the  $\text{C}_2\text{H}_4 \leftarrow \text{NH}_3$  system and estimated to destabilize the transition state by about 2 kcal/mol compared to the structure at  $R_{\text{C}^\alpha-\text{N}} = 3.0$  Å. Of course, the effect of the polarization function is somewhat different for  $[\text{PdF}(\text{C}_2\text{H}_4)]^- \leftarrow \text{NH}_3$ . Nevertheless, the result is considered to be correct in a qualitative sense. The sum of the correction for the activation barrier is about -1 kcal/mol; the MP2 correction (-8 kcal/mol) plus the BSSE correction (+5 kcal/mol) plus the correction by the polarization function (+2 kcal/mol). Although the consideration of these terms is only qualitative, they do not appear to make a sizable contribution. A more detailed examination of these corrections will be carried out in the near future.

## Conclusion

Palladium-assisted nucleophilic attack on a coordinated olefin has been investigated with an ab initio MO method and energy decomposition analysis. The cationic palladium(II)-ethylene complex is proposed as an active species, which agrees with experimental evidence. The activation barrier is calculated to be about 6–8 kcal/mol at the Hartree-Fock level. This value is not expected to change very much when corrected for BSSE and electron correlation effects. The rather low activation barrier seems in accordance with the extreme facility of this reaction. The semiquantitative features of the reaction including changes in geometry and electron distribution are clearly obtained and explained on the basis of orbital mixing. The detailed analysis of those changes suggests that this reaction has a rather early transition state. From the energy decomposition analysis of the interaction between the nucleophile and the palladium-ethylene complex, the origin of the palladium acceleration may be attributed to the large stabilization of ES and FCTPLX and the small destabilization of EX. Thus, the palladium-assisted nucleophilic attack is considered to include characteristics of both frontier control and charge control. From both points of view, neutral and soft ligands favor nucleophilic attack.

**Acknowledgment.** All calculations were carried out by using the Hitac M-200H, M680, and S810 computers of the Computer Center of the Institute for Molecular Science (IMS), through a Joint Studies Program of the IMS. We are grateful to Prof. K. Morokuma and Dr. N. Koga for their interest and generous support and to the Ministry of Education for financial support through Grant-in-Aids.

**Registry No.** 1, 52314-09-7; 2, 108969-67-1; 3, 108969-68-2; 4, 108969-69-3.

(22) Calderazzo, F.; Dell'Amico, D. B. *Inorg. Chem.* **1981**, *20*, 1310. Uson, R.; Fornies, J.; Tomas, M.; Menjón, B. *Organometallics* **1985**, *4*, 1912.

(23) The BSSE value was estimated by the counterpoise method: Boys, S. F.; Bernardi, F. *Mol. Phys.* **1970**, *19*, 553. Ostlund, N. S.; Merrifield, D. L. *Chem. Phys. Lett.* **1976**, *39*, 612.  
 (24) The frozen-core approximation was applied, in which the 1s–3s, 2p–3p, and 3d orbitals of palladium and the 1s orbital of the first-row atoms are included in core orbitals.  
 (25) This type of correction tends to overestimate the BSSE value. However, such an overestimation is not so large here because we discuss only the difference in BSSE between two structures at  $R_{\text{C}^\alpha-\text{N}} = 3.0$  and 2.0 Å.